7. M. B. Zel'man and I. I. Maslennikova, "Effects of resonance interactions of wave perturbations in a boundary layer," Izv. Akad. Nauk SSSR, Mekh. Zhidk. Gaza, No. 4 (1984).
8. V. V. Kozlov, V. Ya. Levchenko, and V. S. Sarik (USA), "Formation of three-dimensional structures during a boundary-layer transition," Preprint, Akad. Nauk SSSR, Sib. Otd. ITPM, No. 10-83, Novosibirsk (1983).
9. M. B. Zel'man, "Development of perturbations of finite intensity in plane-parallel flows," Preprint, Akad. Nauk SSSR, Sib. Otd. ITPM, No. 10-81, Novosibirsk (1981).
10. V. P. Peutov, "A nonstationary critical layer and nonlinear stage development instability in a Poiseuille planar flow pattern," Zh. Prikl. Mekh. Tekh. Fiz., No. 4 (1982).
11. V. N. Zhigulev and A. M. Tumin, Turbulence Initiation [in Russian], Nauka, Novosibirsk (1987).

LONGITUDINAL VORTEX STRUCTURES AND HEAT TRANSFER IN THE REGION OF ATTACHMENT OF A SUPERSONIC TURBULENT BOUNDARY LAYER

E. G. Zaulichnyi and V. M. Trofimov UDC 532.526:536.24

The formation of longitudinal vortex structures in boundary layers of supersonic flows has been observed in experiments conducted by several authors [1-7] who have studied the development of the separation region in plane, axisymmetric, internal, and external flows moving past a body. Both laminar and turbulent flow regimes have been studied in this regard. The development of structures usually termed Taylor–Görtler (T–G) vortices in the neighborhood of the point of attachment in flows after a projection or after a separation point in constricted regions leads to a strictly ordered redistribution of processes involving heat and momentum transfer and their periodic change in the direction transverse to the flow. Under conditions whereby heat transfer is intensified in attachment regions due to an increase in the level of turbulent pulsations [8], the development of secondary flows can lead to additional thermal loads in the regions of their peak values.

From the viewpoint of the development of natural (internal) instabilities in a system, resulting in adaptation, the appearance of T–G vortices is one link in a chain of hierarchical changes in the structure of a boundary layer. It is also significant that the result of loss of stability in the system – the creation of stationary vortices – can be stored in the "memory" of the flow far downstream from the immediate source of the instability.

In the present investigation, we discuss experimental studies of three-dimensional features of flow and heat transfer due to T–G vortices. A second boundary layer of longitudinal structures is observed, the mechanism of its formation not being connected with vortices of the T–G type.

Experimental Conditions. Measurements of pressure field and heat transfer on models of steps were conducted in the T-333 wind tunnel at the Institute of Theoretical and Applied Mechanics (of the Siberian Branch of the Soviet Academy of Sciences) with a jet 304 mm in diameter. The experiments were performed inside an Eifel chamber with the Mach numbers M_1 = 2.0, 3.0, 4.0, and 5.0 for the incoming flow. The range of the Reynolds numbers Re_1 = (30-100)$\cdot 10^6$ m^{-1}, while the range of stagnation pressures $p^* = 180$-1600 kPa. Stagnation temperature T^* varied within the range 260-270 K.

The height of the step (Fig. 1a) located on the plate of width b = 120 mm was h = 6.0, 6.4, and 15.0 mm. The angle of inclination of the face of the step β = 90, 25, and 65°, respectively. The distance from the leading edge of the plate to the vertex of the angle of convergence was 177 mm. We glued a 4-mm-wide vortex generator to the plate 6 mm from its leading edge. The height of the sandy roughness of the generator was 0.2 mm. The characteristic thickness of the boundary layer in the undisturbed flow ahead of the interaction region $\delta_1 \approx 2.1$ mm. Limiter plates (flanges) 30 mm high were installed on the lateral walls of the model to prevent flows in the transverse direction.

Measurements of the local heat-transfer coefficients were made by a modification of the electrocalorimetric method [9] in a complex which included an automatic data processing system

Novosibirsk. Translated from Zhurnal Prikladnoi Mekhaniki i Tekhnicheskoi Fiziki, No. 2, pp. 66-72, March-April, 1991. Original article submitted March 31, 1989; revision submitted August 25, 1989.

 0021-8944/91/3202-0204$12.50

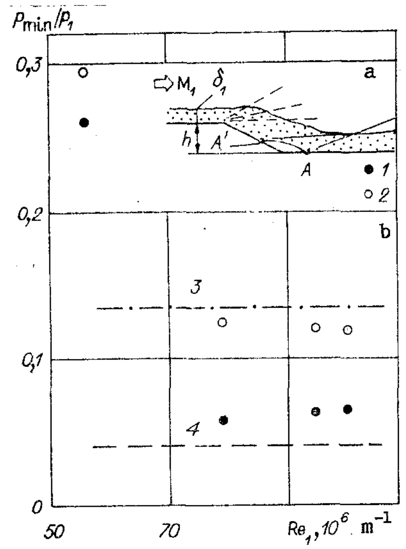

Fig. 1

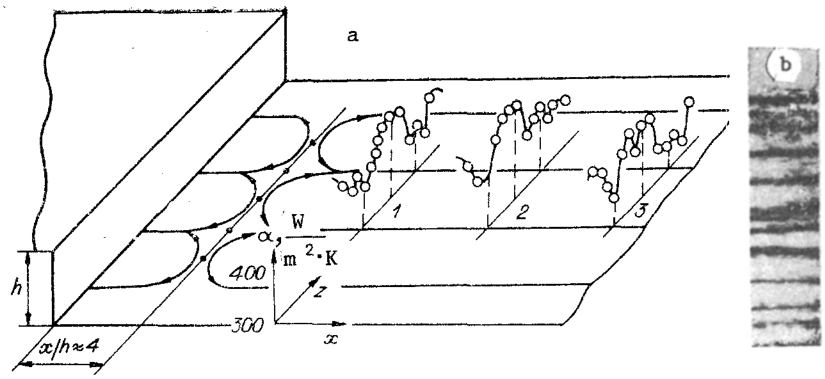

Fig. 2

based on an MERA-60 microcomputer. Measurements of the distributions of pressure on the wall and in the flow were made using integral transducers with a silicon membrane (error no greater than 0.1%). These methods were augmented by visualization of the limiting streamlines and the use of the shadow method. The shadowgraph was also used in conjunction with a telecommunication system to monitor the working flow regimes.

Experimental Results and Discussion. In order to determine the effect of transverse gas flow on the course of the process in the separation region beyond the step, we conducted preliminary tests with and without the limiting plates.

According to the visualization data, when gas flows around a step facing downstream, the boundary layer interacts with rarefaction waves. Here, it reverses at the expansion (see Fig. 1a), separates before the constriction (point A'), and subsequently becomes reattached after the step (point A). Here, it is known [10] that with an increase in the Mach number of the incoming flow, the separation point on an inclined step is shifted downward along the sloping face of the step. We will take the minimum pressure on the inclined face of the step p_{min} as the parameter characterizing aerodynamic expansion and flow separation. An increase in this parameter is an indication of a decrease in the broadening of the flow at the channel expansion and simultaneous displacement of the separation point farther upstream, i.e., it is evidence of an increase in the size of the separation zone. The experimental data in Fig. 1b illustrates the heavy dependence of the parameter p_{min}/p_1 (where p_1 is the pressure in the incoming flow) on the presence of lateral limiter plates. For the test being discussed here, $M_1 = 4.0$. The experimental values of p_{min}/p_1 in the presence of the lateral plates (points 1 in Fig. 1b) at $Re_1 > 70 \cdot 10^6$ approach the theoretical Prandtl–Meyer value (curve 4) for an angle of rotation of the flow equal to the inclination of the step ($\beta = 25°$). Thus, under the given conditions, the flow nearly rotates through the angle of expansion β before the separation point A'. Removal of the side plates (points 2) leads to an increase in the parameter p_{min}/p_1 by a factor of 2 for the same region of Re_1. Here, the parameter approaches the theoretical Korst value [11] for the bottom pressure behind a rectangular step with the same M_1 (curve 3). Thus, transverse flows of gas (the case without lateral limiter plates) significantly distort the pattern of normally two-dimensional flow and induce separation in the longer region. It should be noted that the ratio of the span of the model to the height of the step b/h = 20 turned out to be large enough to eliminate the effect of lateral three-dimensional flows on the central region where the measurements were made. At the same time, it is known that the presence of lateral plates will not affect the pressure diagram on the wall along the symmetry axis of the model for the case of a step turned against the flow [12] if the length of the separation region is less than the span of the model and if the latter is at least five times greater than the height. The conditions of flow past forward- and backward-facing steps obviously differ basically with respect to the extent of the manifestation of three-dimensional flow due to transverse motion of gas. Flow past a backward-facing step can be represented by a scheme with two mass sources, located on the flanks of the separation zone. Flow past a step facing downstream can be represented by a scheme with two sinks at the corresponding points. The presence of the lateral plates eliminates these flow features.

It should be noted that M_1 and Re_1, as well as b/h, are the determining parameters in this case. They determine the intensity of the transverse gas flows.

We applied a soot–oil composition with a volatile component (kerosine) to the surface of the models in order to visualize the limiting streamlines downstream beyond the attachment region. Figure 2 shows the results of the visualization and measurements of heat transfer past a step of the height h = 6 mm. Here, $\beta = 90°$ and $M_1 = 3.0$. Visible to the right are dark bands extending along the flow. These bands correspond to spreading lines formed in the interaction of braid-like longitudinal vortex structures with the wall of the model beyond the flow attachment region. Comparison of the distributions of the heat-transfer coefficients α in Secs. 1-3 (x = 30, 50, and 70 mm from the step) with the visualization pattern shows a correspondence between the heat-transfer minima (the dark lines) and maxima (light lines). A sequence of nodal and saddle points (depicted schematically) is seen at a distance $x/h \simeq 4.0$ from the step. Longitudinal spreading lines (the lines of lower intensity) are distinguishable in the recirculation zone bounded by these points and the base of the step. The presence of the spreading lines is evidence of the existence of vortices in the reverse flow as well. It was noted that the light bands corresponding to the spreading lines are considerably broader than the dark bands. This absence of "symmetry" is also expressed in the fact that the distribution curve for the heat-transfer coefficient is more like a cycloid than a sinusoid.

It should also be pointed out that indications of the existence of T–G vortices were seen with flow past reverse-facing steps under conditions in which flows with a free separation point are realized. The fact that no such indications were observed in previous studies (such as [4]) can be explained by the fact that the inclined-step model used in [4] did not have lateral limiter plates – which altered the conditions of flow past the body.

Experiments conducted on models with steps of different heights showed that the mean spacing of the bands – and, thus, the transverse dimension of the vortex structures – is proportional to the height of the step. It should be recalled that the ratio of the thickness of the boundary layer ahead of the step to its height was considerably less than unity in our experiments. It can be stated that the clear bands (spreading lines) corresponded to sections along the symmetry axis of the model in all of our tests.

One important feature of the limiting-streamline pattern observed in our experiments was the existence of a second field of dark lines between the main lines. The spacing of the dark lines of the second field was 3-4 times smaller than the spacing of the main dark lines. The contrast, regularity, and spacing of the bands are seen to increase with an increase in the Mach number. At $M_1 = 50$, the longitudinal lines of this second field are even more pronounced than the main lines due to T–G vortices. The dark lines of the second field are evidently spreading lines that owe their existence to smaller longitudinal vortices concentrated in the immediate vicinity of the wall.

Several general conclusions can be made from an analysis of the above-obtained distributions of the local heat-transfer coefficient along and across the plate.

1. Large periodic changes in α are seen in the section immediately after the attached layer. The "wavelength" of these changes is on the order of two local thicknesses of the shear layer and corresponds to the mean spacing between the spreading lines; the maxima and minima on the curves depicting the periodic changes in α are stationary and are repeated in different tests with a fixed value of M_1; the indicated changes in α are due to the action of longitudinal T–G vortices.
2. Periodic changes with a smaller relative amplitude and a wavelength $\sim\lambda/3$ are also seen against the background of coarse periodic changes (shown in Fig. 3 are the distributions of α in sections 1-3 (x = 24, 45, and 66 mm from the vertex of the exterior angle of the step) for $M_1 = 4.0$, $Re_1 = 72 \cdot 10^6\ m^{-1}$ and $\beta = 25°$).

It should be noted that the positions of the maxima and minima of the λ-periodic changes in α are not affected by changes in the form of the vortex generator or by variation of the flow parameters before separation. At the same time, the pattern of small-scale changes in α (with the wavelength $\sim\lambda/3$) is shifted as a whole in the transverse direction and varies for different Re_1.

The mean wavelength of the λ-periodic changes in α decreases somewhat with an increase in M_1, and this change correlates with the data from the soot–oil visualization. There is also a decrease in the thickness of the shear layer of the attached flow, since the dimensions of the separation zone beyond the step decrease [10]. This result agrees qualitatively

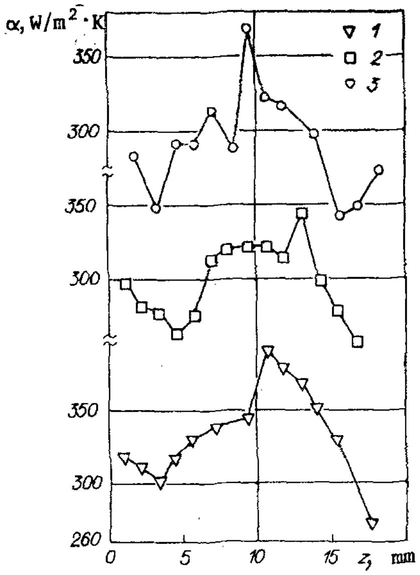

Fig. 3

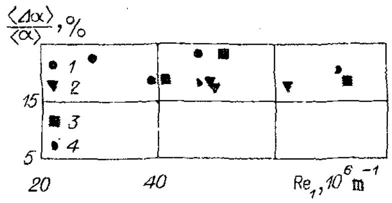

Fig. 4

with the well-known relation obtained by Görtler for an incompressible boundary layer on a concave surface ($\lambda/\delta = 2.5$) [13].

The amplitude of the λ-periodic changes in α recorded in the control section $x = 24$ mm is nearly independent of M_1 and Re_1. Thus, the relative deviation of the heat-transfer coefficients from the values averaged over the span of the model (Fig. 4, where points 1-4 correspond to $M_1 = 2$, 3, 4, and 5) lies within the range 17.5-23.4% throughout the investigated range of M_1 and Re_1. The weak dependence of the amplitude of the changes in α on M_1 was noted in the attachment region behind a rectangular step in [3]. The deviation of α from the mean value in [3] is 10-15%. The amplitude of the changes in α increased particularly dramatically (up to 35%) in tests conducted with artificial irregularities in the form of sinusoidal depressions on the edge of the step. It was established experimentally in [5] that the same effect is obtained by placing a vortex generator in the form of a strip of metal on the edge of the step, with the thickness of this strip being on the order of the displacement thickness in the incoming boundary layer. Except for those noted above, almost none of the published studies contain data from direct measurement of the change in the heat-transfer coefficient after a normal (without irregularities) step. According to [6], the peaks of the heat-transfer rate are no greater than 10-25% above the mean level. At the same time, the estimate made of this quantity on the basis of ablation of the wall material (mass-transfer rate) [2] was 30-40%. In [7], the ablation method was backed up by x-ray diffraction analysis of the material that was in the flow. The estimate of the deviation of the heat-transfer peaks from the mean level turned out to be about 23%. Considering the lack of correspondence between the data obtained by measuring heat- and mass-transfer coefficients, preference should be given to the former due to its greater accuracy. Thus, our results from direct measurement of heat-transfer rate can be considered to agree satisfactorily with the well-known data of other authors. Agreement with other data [1, 7] was also obtained in our measurements of the decay of the changes in heat transfer downstream from the attachment region.

According to the experimental data, the effect of Re_1 also differs for λ- and $\lambda/3$-periodic changes in α. Whereas the former is almost unaffected by Re_1, the situation is complicated in the case of $\lambda/3$-periodic changes. The effect of Re_1 on $\lambda/3$-periodic changes in α is negligible at $M_1 = 4.0$ but is appreciable at $M_1 = 3.0$.

Thus, the results of the heat-transfer measurements and the visualization permit the conclusion that there are two types of longitudinal vortex structures with different mechanisms in the boundary layer beyond the attachment point. As a result, the above determination of $\lambda/3$-periodic structures is somewhat conditional. The visualization showed that the spacing of the $\lambda/3$-periodic structures increases with an increase in M_1. The thickness of the viscous sublayer of the turbulent boundary layer is evidently the characteristic scale of these vortex structures.

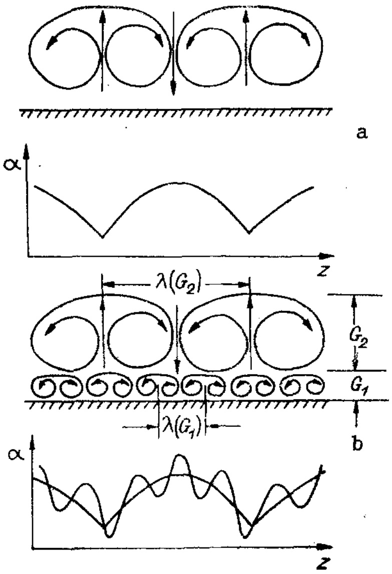

Fig. 5

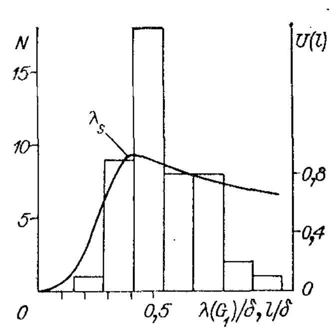

Fig. 6

The presence of new, smaller longitudinal vortices in the boundary layer under the given conditions suggests a need for refinement of the scheme (Fig. 5a) which shows T–G longitudinal structures and their effect on heat transfer. In accordance with the revised scheme for flow past the attachment point (Fig. 5b), the longitudinal vortex structures form two layers. Beginning from the wall, the first layer consists of pairs of G_1-vortices with the mean spacing $\sim\lambda/3$. Located above these vortices is a layer of G_2-vortex pairs with the mean spacing λ. The overall effect of the two layers of vortices of different scales on the rate of heat transfer is the result of the superposition of the effects of each layer separately. It should be mentioned that these representations require additional studies of the fields of the fluctuation characteristics of the flow and the further improvement of optical methods. For example, the three-dimensional visualization in [14] of low-velocity flows on a plate made it possible to establish that two scales of three-dimensional Görtler vortex-waves are formed in a developed turbulent layer as a result of the instability of Tollmien–Schlichting plane waves. It was also established in the same study that these vortex-waves in turn generate small-scale waves, i.e., the process of the development of instability proceeds in cascade fashion from coarser to finer vortex structures. Here, all of the above-examined types of waves exist simultaneously.

It is important to point out that the observed regular (across the flow) and irregular (along the flow) pattern of change in the heat-transfer coefficient due to G_1-vortices (compared to G_2-vortices) correlates with the phenomenon, noted in [14], whereby G_1-vortices rise from the wall region to the upper boundary of the boundary layer. Thus, the behavior of the G_1-vortices is similar to the ordered motions first seen in [15] in the laminar sublayer of the turbulent boundary layer of an incompressible fluid. Instantaneous rates of change in the velocity components u and w across the flow were obtained in the latter study. The measured mean interval between changes is $(0.3\text{-}0.4)\delta$, depending on the longitudinal pressure gradient. Let us compare this data with out data from measurements of the spacing of the G_1-vortices.

Figure 6 shows a histogram depicting the results of analysis of our data on heat transfer. There is a distinct maximum at $\lambda(G_1)/\delta \simeq 0.45$ for the number of maxima N for equal-width segments of the G_1-vortex wavelength (spacing) interval. The results from [15] are shown in the form of the function $U(\ell)$ (curve), which gives the contribution from harmonics with the wavelength ℓ to the change in instantaneous velocity along the span of the model. The maximum of this function is the mean spacing λ_s. It is evident that λ_s is close to the mean spacing of the G_1-vortices. The similar nature of the G_1-vortices and ordered Kline motions [15] is illustrated by the results of a statistical analysis of a large number of experiments. However, reaching a final conclusion as to whether or not the two types of motion are in fact identical will require additional information obtained from more precise measurements.

While the generation of G_1-vortices (or Kline vortices) can be attributed to the generation of turbulence in regions near a wall and the associated property of three-dimensionality [15], the formation of G_2-vortices (or T−G vortices) is connected with the creation of unstable conditions inside shear layers. A criterion for the latter was obtained by Rayleigh [13] for the case of inviscid flow between two coaxial cylinders in the case when the inside cylinder rotates and the outside cylinder remains still. It turns out that the flow is unstable when the peripheral velocity u decreases more rapidly than 1/r as the radius r increases, i.e., when

$$u(r) = \mathrm{const}/r^n \quad (n > 1). \tag{1}$$

The Reynolds numbers are quite large ($Re_1 > 10^7$) in the practically important cases of high-speed flow. If we examine the characteristic types of velocity distributions in different shear layers from the viewpoint of Reyleigh's theoretical finding [13], we find that condition (1) is satisfied near separation points in constrictions and attachment regions after steps. In fact, in this case the distribution of dimensionless velocity in the shear layer is close to that described by the Görtler profile

$$u = 0{,}5\,(1 + \mathrm{erf}\,\eta),\ \text{where}\ \mathrm{erf}\,\eta = \frac{2}{\sqrt{\pi}}\int_0^{\eta} \exp(-\eta^2)\,d\eta, \quad \eta = \sigma y/x$$

(σ is the expansion parameter determined by the Mach number on the outside boundary of the shear layer; for example, in accordance with [11], $\sigma = 12 + 2.76M_e$). Using L'Hospital's rule, it can easily be shown that erf η approaches zero more rapidly than does $1/\eta$ as $\eta \to \infty$:

$$\lim_{\eta\to\infty} \frac{\mathrm{erf}\,\eta}{1/\eta} = \lim_{\eta\to\infty} \frac{2\eta\exp(-\eta^2)}{1/\eta^2} = 0.$$

Thus, it is proven that the Görtler profile satisfies condition (1). At the same time, it is obvious that (1) is not satisfied for all types of flows in a turbulent boundary layer described by a power function. This is because the exponent of the function does not exceed unity in such flows. As a result, of all of the above-examined examples of turbulent shear flows, it is only in the neighborhood of separation and attachment points that T−G vortices can be generated. Here, we have in mind those separation points at which $dp/dx > 0$ (the latter is satisfied for certain at attachment points). The conclusion just stated is consistent with well-known empirical data on the formation of longitudinal vortex structures and our measurements. However, it should be noted that vortex structures of a different type [16] will develop in certain types of separated flows − such as on cones with a discontinuous generatrix.

Measurements of different flow characteristics, including the heat-transfer coefficient, show that T−G vortices exist along with the above-observed longitudinal structures of thin boundary layers as a steady secondary flow which acts to redistribute transport processes.

LITERATURE CITED

1. V. N. Brazhko, "Periodic structure of flow and heat transfer in the region of attachment of supersonic flows," Uch. Zap. TsAGI, 10, No. 2 (1979).
2. G. F. Glotov and É. K. Moroz, "Longitudinal eddies in supersonic flows with separation zones," Uch. Zap. TsAGI, 8, No. 4 (1977).
3. V. I. Khonichev, A. V. Mezentsev, and I. K. Ermolaev, "Heat transfer in the region of attachment of a supersonic turbulent boundary layer with longitudinal vortex structures," in: Heat and Mass Transfer [in Russian], Part 1, Minsk (1988).
4. A. A. Zheltovodov, L. Ch. Mekler, and É. Kh. Shilein, "Features of the development of separated flows in constrictions behind rarefaction waves," Preprint, Akad. Nauk Sib. Otd. IPTM, No. 10−87, Novosibirsk (1987).
5. V. M. Trofimov, "Study of gasdynamics and mass transfer in turbulent separated flows," Engineering Sciences Candidate Dissertation, Novosibirsk (1987).
6. Inger, "Spatial features of heat- and mass-transfer processes in the region of attachment of a high-speed flow," AIAA J., 15, No. 3 (1977).
7. A. V. Mezentsev, V. I. Khonichev, S. M. Shebanov, and I. K. Ermolaev, "Spatial features of heat and mass transfer in the ablating surface layer of high-enthalpy channels," Teplomassoobmen-VII, Vol. 3, Minsk (1984).
8. E. G. Zaulichnyi and V. M. Trofimov, "Study of heat transfer in separated regions of a supersonic flow in a de Laval nozzle," Zh. Prikl. Mekh. Tekh. Fiz., No. 1 (1986).

9. V. N. Zaikovskii, E. G. Zaulichnyi, B. M. Melamed, and Yu. M. Senov, "Experimental study of local heat- and mass-transfer coefficients on the walls of a valve assembly," Zh. Prikl. Mekh. Tekh. Fiz., No. 2 (1982).
10. A. A. Zheltovodov, E. G. Zaulichnyi, V. M. Trofimov, and V. N. Yakovlev, "Study of heat transfer and turbulence in compressible separated flows," Preprint, Akad. Nauk Sib. ITPM, No. 22-87, Novosibirsk (1987).
11. P. Chen, Separated Flows [Russian translation], Vols. 1-3, Mir, Moscow (1972-1973).
12. Zukoski, "Separation of a turbulent boundary layer before a step," AIAA J., 5, No. 10 (1967).
13. G. Schlichting, Boundary Layer Theory [Russian translation], Nauka, Moscow (1974).
14. S. Taneda, "The main structure of turbulent boundary layers," J. Phys. Soc. Jpn., 52, No. 12 (1983).
15. S. I. Kline, W. C. Reynolds, F. A. Schraub, and P. W. Runstadler, "The structure of boundary layers," J. Fluid Mech., 30, Part 4 (1967).
16. Redding, Hunter, Erickson, and Leff, "Absence of axisymmetry in a separated flow," AIAA J., 7, No. 7 (1969).

STABILITY OF TWO-DIMENSIONAL TRAVELING WAVES ON A VERTICALLY DRAINING LIQUID FILM TO THREE-DIMENSIONAL PERTURBATIONS

Yu. Ya. Trifonov

UDC 532.51

It is known that for practically all Reynolds numbers waves exist on the surface of a liquid layer draining along a vertical tube. This is because the flow of a film with a smooth free surface is unstable [1]. Unless special measures are taken (such as the creation of uniform conditions around the perimeter of the tube at the inlet) the waves are three-dimensional and irregular [2] and are extremely sensitive to external perturbations. Hence the theoretical or experimental study of a draining film is very difficult.

The wave flow can be regularized by applying pulsations to the flow rate or by creating uniform conditions at the flow inlet [2, 3]. Then there exists a region of two-dimensional (annular) regular waves whose length depends strongly on the properties of the liquid and the flow rate [3], and which evolves into three-dimensional flow [3].

By superimposing pulsations of different frequencies, two-dimensional waves of different lengths can be generated. There exist two types of waves with very different properties: quasiharmonic and solitary waves [2, 3]. The system of equations of [6] for the instantaneous thickness and flow rate of the liquid was used in [4, 5] to calculate different two-dimensional nonlinear steady traveling waves. Some of these wave processes were found to be in good quantitative agreement with experiment. The stability of these wave processes to plane infinitesimal perturbations was studied in [7-9] by means of bifurcation analysis. Two types of waves were preferred in the sense of stability. These preferred waves will be referred to as belonging to the first and second families, and they correspond to the quasiharmonic and solitary waves observed experimentally.

The equations of [6] were extended to the case of three-dimensional perturbations in [10] by averaging the equations of motion in the direction perpendicular to the layer (the y direction) and assuming certain velocity profiles in the x direction (along the gravitational acceleration vector) and in the z direction. These equations can be written in the form

$$\frac{\partial q}{\partial t}+1{,}2\left(\frac{\partial}{\partial x}\frac{q^2}{h}+\frac{\partial}{\partial z}\frac{qQ}{h}\right)=-\frac{3\nu q}{h^2}+gh+\frac{\sigma h}{\rho}\left(\frac{\partial^3 h}{\partial x^3}+\frac{\partial^3 h}{\partial x\,\partial z^2}\right),$$

Novosibirsk. Translated from Zhurnal Prikladnoi Mekhaniki i Tekhnicheskoi Fiziki, No. 2, pp. 72-77, March-April, 1991. Original article submitted March 28, 1989; revision submitted December 21, 1989.

